STRAIN AND DAMAGE SENSING DURING LOADING OF CARBON NANOTUBE DOPED COMPOSITES

S.P. Fernberg, R. Joffe, G. Nilsson
Swerea SICOMP AB
P.O. Box 271, 941 27 PITEÅ, Sweden
Patrik.Fernberg@swerea.se

SUMMARY

This work explores the possibility to use resistance changes in a carbon nanotube (CNT) doped composites to monitor deformations and damage. Most other studies in the field are done on simplified uniaxial loading whereas current work also evaluates the possibilities to monitor strain in more complex loading case, such as bending.

Keywords: carbon nanotubes, multi-scale composite, strain sensing, damage detection, electrical resistance

INTRODUCTION

The current report presents results and analysis from studies of the structural and electrical response of carbon nanotube doped fiber composites subjected to various forms of mechanical loading. It has been shown in previous studies [1-3] that the electrical resistance of a CNT doped composite changes when it is mechanically loaded. It is known that the variations of electrical resistance originate from (a) geometrical changes of the specimen, (b) piezoresistive material response and (c) accumulation of discrete damage. From a conceptual point of view one can use the simple Ohm's law for a slender conductor to illustrate qualitatively how beforehand mentioned mechanisms influence the specimen resistance:

$$R = \rho \frac{l}{A} \tag{1}$$

where, R - resistance, ρ - resistivity, l - length and A - cross sectional area. Loading in tension implies that l increases while A decreases with applied strain ε. R in Eqn. 1 will hence increase upon such loading. It was also shown that CNT nanocomposites have a piezoelastic nature i.e. ρ in Eqn. 1 increases if the material is subjected to tensile strain. Resistance increase observed during loading in tension will thus be magnified by the piezoresistive contribution. Moreover, one can say that damage, occurring in the form of cracking or in the form of disruption of the conductive CNT -network, contributes to an increasing resistance since it can be interpreted and viewed as if the effective length (l) in Eqn. 1 increases. The above reasoning is very intuitive and obvious for the case of unidirectional tension loading of a slender test specimen. This is probably a reason why a majority of the results presented in literature deals with this type of loading. In real structures the loading conditions and geometries are usually more complex. They often have complicated 2D or 3D shapes which allow electrical currents to take complex pathways that are difficult to intuitively predict. Another degree of complexity is added because some parts of the structure are loaded in compression while others are loaded in tension. Resistance may hence increase due to piezoresistivity in certain volumes whereas others remain unchanged or decrease.

In the current report we present results where electrical resistance changes of CNT-doped composites are characterized for various loading conditions and specimen geometries. Results from tensile loading experiments are compared with results from standard type of flexural loading (e.g. 3-point bending) as well as with results from bending tests of plates. The ultimate objective of the work is to assess, evaluate and demonstrate the potential to use resistance mapping as a non-destructive method for strain and damage measurements in real composite structures.

THEORY

A simple model for resistance change during bending of piezoresistive beams

A simple theoretical model with ambition to support the evaluation of experimental results was derived. The model simulates and calculates expected resistance changes due to the combined effect of geometrical changes and piezoresistivity during loading in bending. The model relies on some simple but realistic assumptions about strain distribution and geometry. These assumptions are summarized in Figure 1.

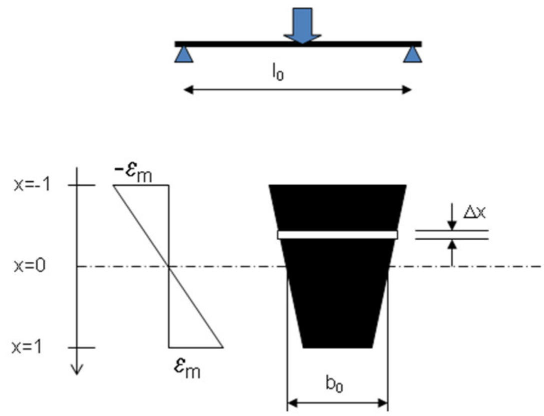

Figure 1. Assumed geometry and strain distribution during bending

The resistance of a small slice of the beam expressed in terms of Ohm's law (c.f. Eqn 1) is given by

$$\Delta R = \rho \frac{l(x)}{\Delta A(x)} = \rho \frac{l(x)}{\Delta x(x) b(x)} . \tag{2}$$

The geometry of beam as function of distance from neutral axis is given by

$$b(x) = b_0(1 - \nu\varepsilon) = l_0(1 - \nu\varepsilon_m x) \tag{3}$$

$$l(x) = l_0(1 + \varepsilon) = l_0(1 + \varepsilon_m x) \tag{4}$$

$$\Delta x(x) = \Delta x(1-\nu\varepsilon) = \Delta x(1-\nu\varepsilon_m x). \tag{5}$$

Insertion of (3) – (5) in (2) yields in

$$\Delta R = \frac{1}{\Delta x}\rho\frac{l_0(1+\varepsilon_m x)}{b_0(1-\nu\varepsilon_m x)^2}. \tag{6}$$

By taking the inverse of Eqn 6 one obtains (cf. impedance of resistances in parallel)

$$\frac{1}{\Delta R} = \Delta H = f(x)\Delta x \tag{7}$$

where

$$f(x) = \frac{b_0(1-\nu\varepsilon_m x)^2}{\rho l_0(1+\varepsilon_m x)}. \tag{8}$$

Consider the limit value when a slice becomes infinitesimal small

$$\frac{\Delta H}{\Delta x} = f(x) \rightarrow \frac{\partial H}{\partial x} = f(x) \text{ as } \Delta x \rightarrow 0 \tag{9}$$

Eqn 9 is separable PDE that can be solved by

$$\frac{1}{R} = H = \int_{-1}^{1} f(x)dx = \int_{-1}^{1}\frac{b_0(1-\nu\varepsilon_m x)^2}{\rho l_0(1+\varepsilon_m x)}dx. \tag{10}$$

Maple-software is used to solve the expression in Eqn. 10. This gives the value of resistance changes with applied strain if no piezoresisitivity is considered.

$$R = -\frac{\rho l_0\varepsilon_m}{b_0} \bigg/ h(\varepsilon_m, \nu) \tag{11}$$

where

$$\begin{aligned} h(\varepsilon_m,\nu) &= 4\varepsilon_m\nu - 2\ln(1+\varepsilon_m)\nu - \ln(1+\varepsilon_m) + 2\nu^2\varepsilon_m \ldots \\ &\ldots - \ln(1-\varepsilon_m)\nu + \ln(1-\varepsilon_m) + \ln(1-\varepsilon_m)\nu^2 \end{aligned}. \tag{12}$$

By assuming a linear relation between resistivity and applied strain one may derive a model that includes effects from a piezoresistive matrix i.e.

$$\rho = \rho_0(1+k\varepsilon) = \rho_0(1+k\varepsilon_m x). \tag{13}$$

Replacement of the constant resistivity in Eqn. 10 with the behaviour described by Eqn. 12 gives eventually an expression for resistance changes with applied strain if linear piezoresisitive behaviour is assumed.

$$R = -\frac{\rho l_0 k^2 (1-k)\varepsilon_m}{b_0} \Big/ g(\varepsilon_m, \nu, k) \tag{14}$$

where

$$\begin{aligned} g(\varepsilon_m,\nu,k) &= -\ln(1+\varepsilon_m)\nu^2k^2 + 2\ln(1+k\varepsilon_m)\nu k - 2\nu^2\varepsilon_m k + 2\nu^2\varepsilon_m k^2 - \ln(1+\varepsilon_m)k^2 \ldots \\ &\ldots - 2\ln(1+\varepsilon_m)\nu k^2 + \ln(1+k\varepsilon_m)k^2 + \ln(1+k\varepsilon_m)\nu^2 + \ln(1-\varepsilon_m)\nu^2k^2 - 2\ln(1-k\varepsilon_m)\nu k \ldots \\ &\ldots + \ln(1-\varepsilon_m)k^2 + 2\ln(1-\varepsilon_m)\nu k^2 - \ln(1-k\varepsilon_m)k^2 - \ln(1-k\varepsilon_m)\nu^2 \end{aligned} \tag{15}$$

Flexural strain in CNT-doped laminates with offsetting glass fibre laminates

In the experimental part of the work we are using – what we consider as so-called "dummy" glass fibre/epoxy laminates – in order to avoid simultaneous presence of both, tensile and compressive stresses when a laminate subjected to bending. The "dummy" material is an electrically insulating laminate that is glued on one side of a CNT-doped composite. The neutral axis of the whole structure is shifted and the doped laminate is either solely subjected to tensile or compressive stresses, depending on location of the additional glass fibre plate. The configuration is useful for varying the loading but has the limitation that it imparts difficulties when analysing results if only load and displacement is registered during the experiments. We have used Classical Laminate Theory (CLT) for calculations to relate applied load with the maximum in-plane strain, ε_m. The final results of these calculation was proportionality constants C_ε , presented in Table 1, which related applied lateral load F to the maximum strain ε_m in the outer layer of the tested laminates.

Table 1 Configurations, dimensions and calibration results from elastic analysis

Configuration	*Type*	*Loading of doped composite*	*height [mm]*	*width [mm]*	*Span length [mm]*	*C_ε [%/N]*
$(0/90)_{6T}\,(0)_{6T}$	Plate	Tension	8	100	100	$8.1\cdot10^{-5}$
$(0)_{6T}\,(0/90)_{6T}$	Plate	Compression	8	100	100	$-8.6\cdot10^{-5}$
$(0/90)_{6T}(0)_{6T}$	stripe	Tension	8	7.5	61.5	$6.6\cdot10^{-4}$
$(0)_{6T}(0/90)_{6T}$	stripe	Compression	8	7.5	61.5	$-7.1\cdot10^{-4}$
$(0/90)_{6T}\,(90)_{6T}$	stripe	Tension	8	7.5	61.5	$2.23\cdot10^{-3}$
$(90)_{6T}\,(0/90)_{6T}$	stripe	Compression	8	7.5	61.5	$-2.28\cdot10^{-3}$

MATERIALS

Unidirectional non-crimp glass fibre fabrics, Devold T600-E05 with nominal surface weight of 600 g/m^2, were used. The resin is an anhydride cured epoxy system Araldite LY556/Aradur HY 917/Accelerator DY 070 mixed in the ratio: 100/90/1.5. Multiwalled CNT supplied by Arkema was used as CNT-additive. A batch with CNT premixed in base resin, also supplied by Arkema, was also evaluated. The premixed resin was designated GRAPHISTRENGTH CS1-015. The GRAPHISTRENGTH material contained 1.5% CNT and has an epoxy content of 5.22 – 5.37 Eq/kg. The procedure used for obtaining the correct amount of CNT (0.3% in our experiments) was to dilute GRAPHISTRENGTH in to LY556 in the proper proportions while still using the same curing agent and accelerator. Three different methods for obtaining well dispersed nanocomposite resin was considered a) calendaring using a three roll mill as described in e.g. [4] b) ultrasonication according to procedures used in previous work [1] and c) a simple shear mixing procedure using a laboratory mixer. The composites were manufactured using RTM-technique and the fibre volume fraction was intentionally kept at a low level, at around $V_f = 40$ %, to avoid problems with filtering of CNT during mould filling. All materials are cured for at least 14 hours at 80°C followed by a 4 hours post cure at 140°C.

Table 2 Materials studied

Label	Resin	Lay-up	w_{CNT}[%]	Dispersion method	V_f[%]
P1	LY556	$[0°]_5$	0.3	Calendaring	39%
P2	LY556	$[0°]_6$	0.3	Sonication	40%
P3	CS1-015/LY556	$[0°]_6$	0.3	Premixed batch	40%

EXPERIMENTAL

Bending experiments

The plates, in form of beams (stripes) and plates are tested in different variants of bending loading. A photograph of a plate specimen is showed in Figure 2. Beam specimens can be seen in the background in the same picture. The beams have a span length of about 61.5 mm and a width of 7.5 mm. A majority of the samples have a glass fibre plate adhesively bonded to one side. The glass fibre plate is used to deliberately shift the neutral axis of the beam. A majority of the electrically conductive material thus will be loaded in tension if the CNT-doped material is placed downwards and in compression when one turns the specimen in the other direction.

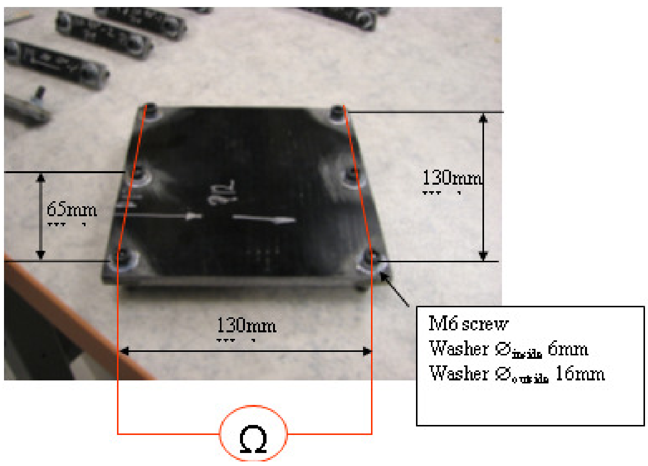

Figure 2. Configuration and geometry of plate sample

Mechanical testing was performed using an Instron 5801 servo hydraulic testing machine with a 100 kN load cell. All measurements of electrical resistance are made with a Keithley 2100 DMM in the four wires mode. The electrical connections are prepared by drilling holes in which silver paint is applied. Finally a steel bolt is attached through the samples and the electrical contacts are applied to the bolts.

RESULTS & DISCUSSION

Initial resistances, R_0

Values of initial resistances R_0 of each individual sample are presented in Table 3. R_0 appear to be higher in the direction perpendicular to the fibres (2 to 20 times higher). We also notice some differences between different plates (P1 to P3) although they still have values in the same order of magnitude. It is to our opinion not possible to state any systematic difference between different materials.

Table 3 Initial resistance, R_0 [kΩ], of samples subjected to bending tests

Material	Beam 0º-tension (Figure 3)	Beam 0º-compres. (Figure 5)	Beam 90º-tension (Figure 4)	Beam 90º-compres. (Figure 6)	Plate 0º-tension (Figure 7)
P1	134.1	136.8	2802.5	1413.5	71.9
P2	316.6	394.8	845.9	1318.8	102.1
P3	171.5	56.8	1094.1	1727.8	31.2

Beams in tension

Results from bending tests with CNT-doped materials placed on the lower side of the beams are presented in Figure 3 and Figure 4. The filled markers shows values obtained when the samples are loaded to a level corresponding to a certain calculated strain level. The open markers are resistances registered upon unloading the specimen. We notice from that resistance increases with increasing tensile strain. This is in agreement with previous observations [1]. The increase is very small for small loading levels. Larger changes are registered at higher strains, above $\varepsilon_{m,T} = 1.5\%$.

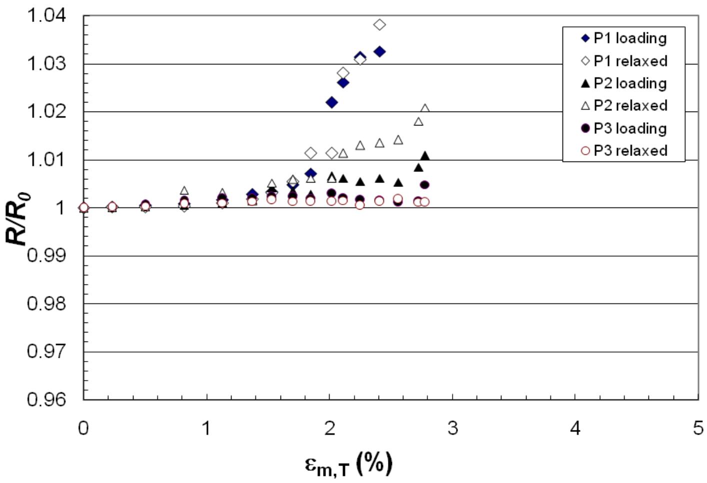

Figure 3. Resistance changes of CNT-doped UD-material in tension, fibres aligned in direction of beam (0º-direction).

In Figure 3 we notice that larger resistance change appears above 1.5% strain. This can be taken as indication that the materials starts to accumulate damage. The magnitude of resistance change above 1.5% varies a lot between individual samples. At this stage we have no solid explanation for this, but one can speculate that it is a consequence of sample-to-sample variations (type of damage, magnitude of damage etc.). A similar behaviour is observed for materials loaded perpendicular to the fibre direction in Figure 4 although there appears to be lower tendency to develop permanent resistance changes for these specimens.

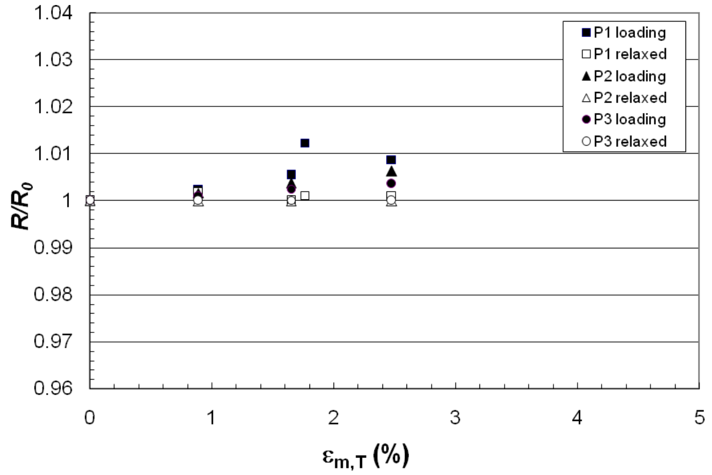

Figure 4. Resistance changes of CNT-doped UD-material in tension, fibres aligned perpendicular with beam (90º-direction).

Beams in compression

Results from bending tests with CNT composites positioned on the compression side are presented in Figure 5 and Figure 6. The filled markers in the plots are values obtained when the samples are loaded and the open markers are registered after unloading. At low strain level it appears that the resistance decrease with increasing compressive strain.

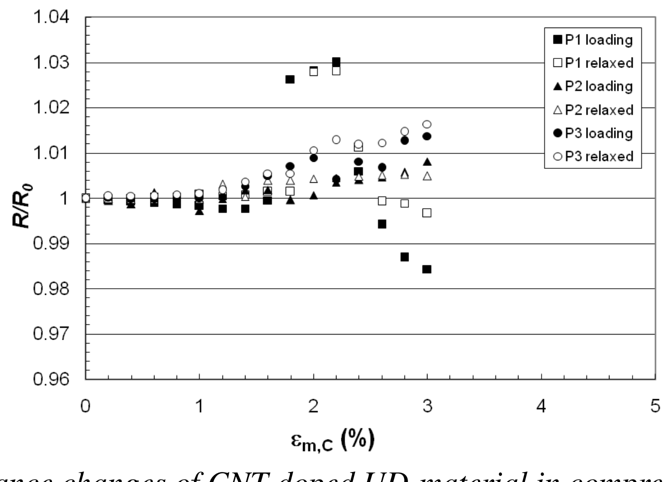

Figure 5. Resistance changes of CNT-doped UD-material in compression fibres aligned in the direction of beam (0º-direction).

The changes are however small, in particular for the specimen loaded in 0º-direction. Upon increasing the strain further we obtain a significant difference in the response, the resistance of specimens loaded perpendicular with the fibres continues to decrease.

These resistances also appear to return to their original values. This is taken as evidence that no damage is accumulated in these specimens. Material loaded in the 0º-direction behaves differently, the resistance starts to increase at about $\varepsilon_{m,C}$ = 1%. The increase is noticed both in the deformed and in the undeformed specimens. Our interpretation is that the specimen starts to develop damage at this stage. This damage interrupts the conductive pathway through the specimen and yields in an increasing resistance. This increase in resistance is much stronger than any resistance reduction due to piezoresistivity. An irregular behaviour occurs at compressive strains above about $\varepsilon_{m,C}$ = 1%, two samples continue to have an increasing resistance whereas one decrease.

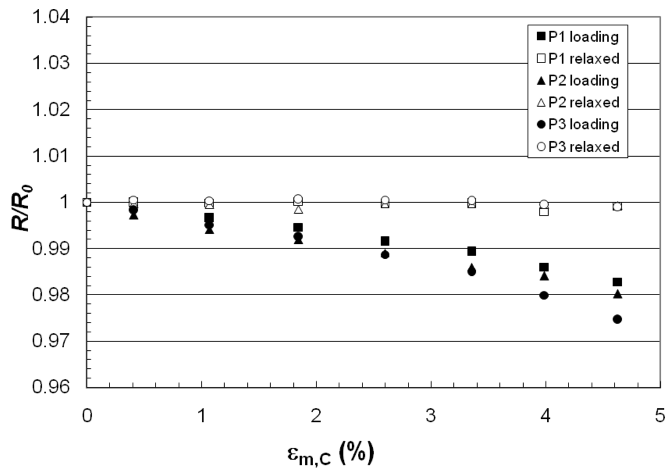

Figure 6. Resistance changes of CNT-doped UD-material in compression, fibres aligned perpendicular to the direction of beam (90º-direction).

Beams in compression and tension

Experiments were also performed on beams and plates made directly from P1-P3 i.e. without any dummy glass fibre laminates glued to the specimen. In these specimen one obtain a strain distribution very similar to the assumed strains presented in Figure 1. Our experimental results confirm that compression and tension contribution in practice cancels out the resistance change, we were hence not able to measure any resistance change.

Plate in tension

One sample, shown in Figure 2, was significantly wider than the other. The plate was supported at the edges and loaded by a line load. The CNT-doped material was subjected to tension loading. Results from the experiment are presented in Figure 7. One notices a general increase of resistance with increasing loading. One should notice that the scale in Figure 7 is different than in previous figures, thus both a smaller strain and resistance change interval is considered. Generally the result in Figure 7 is in agreement with the response at low strains in Figure 3. The resistance increase with increasing strain. Residual resistance, after unloading, seems to increase at the same rate as the loaded samples. This is similar to the behaviour observed for beams tested in tension and in the fibre direction. This gives us reason to conclude that damage appears to be the dominating mechanism causing resistance changes in this mode of loading.

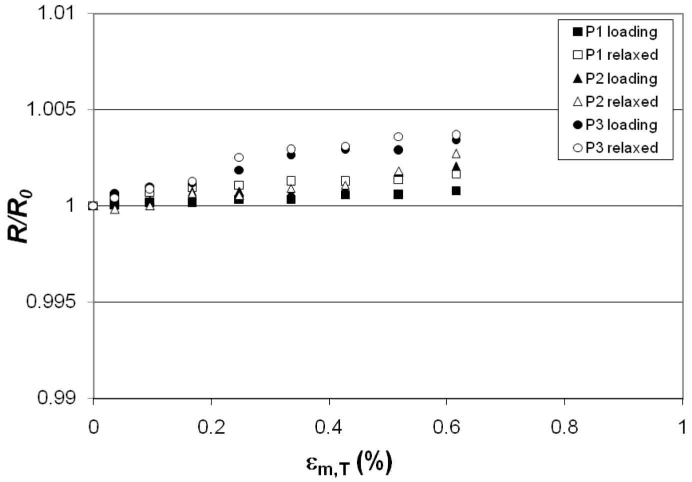

Figure 7. Resistance changes of CNT-doped UD-material: doped material placed on tension side, fibres aligned in the direction of the beam deflection (0º-direction).

Evaluation of theoretical beam bending model

A parametric study based on Equations 4-6 was performed. A Poisson ratio, $\nu = 0.35$ and a value of the constant, *k*= 2, was used in the calculations. The value was obtained based on experimental results obtained in previous work [1]. Figure 8 shows the results obtained for bending.

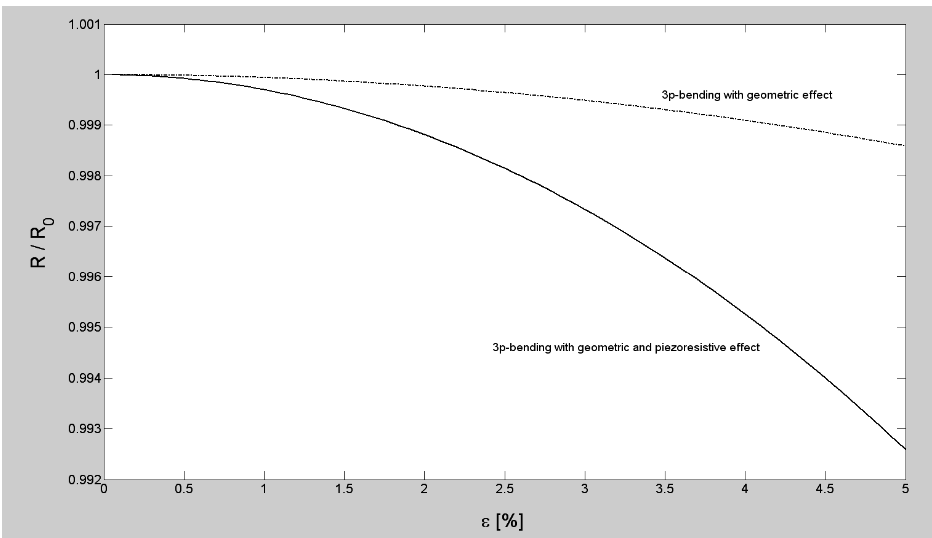

Figure 8. Parametric study: Resistance changes – from Eqn. 4 and 5 – vs. $\varepsilon\,(\varepsilon = \varepsilon_m)$

Two cases are considered: the first one (dotted line) is only considering the geometrical effects whereas the solid line includes both geometrical and piezoresisitive effects. One notice that the resistance decreases with increasing strain in both cases. Thus the parts of the beam that is loaded with compressive loads are dominating (short-circuiting) over the parts that are in tension. The decrease is many times stronger if piezoresistivity also is considered to contribute. One can hence expect an amplified resistance change for beams made from piezoresistive material. If one plots the model results from bending in the same graph as experimentally determined values from loading in pure tension one sees that that the resistance change is many times stronger in the case of tensile loading only. This is no surprise, large part of the beam is in compression during bending loading and this implies, with the current model, that resistance decrease. The theoretical study clearly shows that a much smaller sensitivity to applied strain is expected in a bending experiment than for a tensile test. The theory supports the experimental observations that only small changes due to piezoresisitvity can be observed in the case of loading in bending. It also supports the observation that a decrease in resistance can be observed in the case of compression loading whereas tensile loading implies resistance increase.

CONCLUSIONS

An experimental study was performed where the resistance changes upon deformation of CNT-doped composites was studied and analyzed. Insulating glass fibre plates were glued to some of the samples to promote either tensile or compressive loading. Two different mechanisms were responsible for the changes in resistance: 1) piezoresitivity of the CNT-doped matrix; and 2) damage accumulation. It was experimentally observed that piezoresisitvity either gives a resistance increase or decrease. We conclude that resistance decrease upon compression loading and increase upon tension loading. We notice that the influence of damage is generally that resistance increase. Accumulation of damage appeared to influence specimen loaded in the fibre direction to a larger extent. This caused the resistance to increase in most of the cases for these specimens. It was not possible to measure with confidence any resistance changes in specimens which were subjected to bending experiments (without offsetting glass fibre plates). Any resistance changes were cancelled out since about half of the specimen is in tension and the other in compression. The observed behaviour was analyzed and confirmed by analytical modelling efforts.

ACKNOWLEDGMENTS

This work was performed within a research project, NOESIS, ”Aerospace nanotube hybrid composite structures with sensing and actuating capabilities”, funded by the European Community, Contract no. 516150

References

1. Fernberg P, Nilsson G, Joffe R, Piezoresistive performance of long fibre composites with carbon nanotube doped matrix, in press *Journal of Intelligent Material Systems and Structure*
2. Thostensson ET, Chou TW, Carbon nanotube networks: sensing of distributed strain and damage for life prediction and self healing, Adv Mater 2006;18:2837-2841
3. Fiedler B, Gojny, FH, Wichmann MHG, Bauhofer W, Schulte K, Can carbon nanotubes be used to sense damage in composites?, *Annales de Chimie (Science des Materiaux),* 2004;29:81-94.
4. Gojny FH, Wichmann MHG, Köpke U, Fiedler B, Schulte K. Carbon nanotube-reinforced epoxy-composites—enhanced stiffness and fracture toughness at low nanotube contents. Composites Science and Technology, 2004;64:2363–71.